Transactions of the Materials Research Society of Japan 29[4] 1211-1214 (2004)

Ferroelectric behavior in $SrZrO_3/SrTiO_3$ Artificial Superlattices

Takakiyo Harigai, Daisuke Tanaka, Song-Min Nam, Hirofumi Kakemoto, Satoshi Wada, and Takaaki Tsurumi

Department of Metallurgy and Ceramics Science, Graduate School of Science and Engineering, Tokyo Institute of Technology, 2-12-1 Ookayama, Meguro-ku, Tokyo 152-8552, Japan

Fax: 81-03-5734-2829, e-mail: ttsurumi@ceram.titech.ac.jp

$SrZrO_3/SrTiO_3$ (SZO/STO) artificial superlattices were fabricated on STO substrates by the molecular beam epitaxy process. The stacking periodicity of SZO and STO was varied from 1 unit cell to 40 unit cells, and the total thickness was fixed at 80 unit cells. In-situ reflection high-energy electron diffraction and x-ray diffraction clearly shows the formation of the superlattice structure. Dielectric properties were measured using interdigital electrodes frequency up to 110 MHz, and dielectric relaxation was observed in the $[(SZO)_1/(STO)_1]_{40}$ and $[(SZO)_{10}/(STO)_{10}]_4$ superlattices in the low frequency domain. Dielectric permittivities of all superlattices were over 10,000 at 110 MHz. The measurement results of Q-V hysteresis shows that each of SZO and STO, which constitute the superlattice, was paraelectricity, although, the superlattice which they laminated induced ferroelectricity.

Keyword: $SrZrO_3$, $SrTiO_3$, perovskite compound, artificial superlattice, dielectric property, ferroelectricity

1. INTRODUCTION

Artificial superlattices of oxide materials are of interest in numerous applications as new electronic devices because the superlattices have the potential to drastically improve material properties or to show unknown functionality. And the bulk materials with the perovskite-type structure exhibit various physical properties, such as ferroelectricity, superconductivity and so on. Therefore, the perovskite-type solid-solution thin films have been intensively investigated in the oxide materials. Artificial superlattices which laminated the perovskite-type materials of the different characteristics at an atomic level are expected that it is one of the most interesting systems in research of the oxide superlattices.

Some researches[1-4] concerning $BaTiO_3/SrTiO_3$ (BTO/STO) system have succeeded in fabricating artificial superlattices, and their superlattices show different behaviors from solid solutions of BTO and STO. In the our previous studies[5,6], dielectric properties of several kinds of BTO/STO superlattices were measured. As a result, it was clarified that the dielectric permittivity of BTO/STO superlattices along the film plane depended on the stacking period of superlattices. The superlattices with the periodicity of 10 unit cells showed a maximum permittivity above 30,000, which was almost independent from frequency up to 110 MHz. The refractive index of superlattices measured with a spectroscopic ellipsometer also showed the highest value in the superlattice consists of the 10-periodic structures. This indicated that the structure of superlattices affected not only the ionic polarization but also the electronic polarization. The origin of the high dielectric permittivity has not been clearly understood at present. To elucidate the origin of some unique properties observed in the superlattices, it is required to study the relationship between the structure and the material properties using various type artificial superlattices, such as the ferroelectric/paraelectric combination like the case of BTO/STO, and also the ferroelectric/ferroelectric or the paraelectric/paraelectric combination.

In this study, we focused on the paraelectric/paraelectric combination in the perovskite-type superlattices and fabricated $SrZrO_3$(SZO)/$SrTiO_3$(STO) artificial superlattices. It is expected that properties of this superlattice were not influenced by the ferroelectricity of materials themselves, but by the effect of lattice distortion induced in the superlattice structure.

2. EXPERIMENT

2.1. Growth of the superlattices

The SZO/STO superlattices were fabricated on STO(001) single crystals by the molecular beam epitaxy (MBE) method at a substrate temperature of 600°C. Zirconium and titanium metals were evaporated from the electron-beam guns, and strontium metal was evaporated from the Knudsen cell. Electron cyclotron resonance plasma was irradiated on the surfaces of the growing films and the working pressure in the vacuum chamber, 10^{-6} Torr. The structure of prepared superlattices was represented by a formula $(SZO)_m/(STO)_m$, where the subscript m indicates the period of layers (m=1, 10, 20, and 40). The total thickness of the multilayered films was fixed at 80 unit cells of the primitive perovskite lattice.

Crystallographic orientation and crystallinity of the SZO/STO superlattices were analyzed by reflection high-energy electron diffraction (RHEED) and normal θ-2θ scan mode x-ray diffraction (XRD).

2.2. Dielectric measurements

Dielectric properties of oxide superlattices are usually measured using conductive oxide substrates as a bottom electrode. In our previous studies, we first used conductive Nb-doped STO single crystals as a bottom electrode but reliable results could not be obtained. Because it was found that the leakage current of the film on the Nb-doped STO substrate was much lager than that on the pure STO substrate. So, we formed interdigital electrodes on a film deposited on the pure STO substrate.

Interdigital electrodes were formed by the electron beam lithography technique and the lift-off method. The finger width of this electrode was 5μm and the number of the finger pairs was five. The thickness of Au-sputtered electrodes was approximately 60 nm, and the resistivity of interdigital electrodes 7.4×10^{-6} Ωcm was measured by the dc four-probes method using a RESITEST8200 (Toyo Corp., Japan).

The capacitance and the complex admittance of superlattices were measured at room temperature by an impedance analyzer (Agilent, 4294A) at frequencies from 1 kHz to 110 MHz. For the accurate measurement of impedance at a wide frequency range, a four-terminal pair configuration was employed, and open/short/load calibration was performed using an impedance standard substrate (Cascade Microtech). In addition, Q-V hysteresis curves were measured using the standardized ferroelectric test system (Radiant Tech., RT-66A).

The Farnell theory[7] has been used to calculate the dielectric constant of the film with the interdigital electrode structure, but it is not suitable for the analysis of ultra-thin films like superlattices. Therefore, we used commercial high-frequency planar analysis software (Sonnet em) to design an interdigital electrode pattern and to calculate the dielectric permittivity from the measured complex admittance of the superlattices.

3. RESULTS AND DISCUSSION

3.1. Structure of superlattices

Figure 1(a), 1(b) show a typical RHEED pattern and a trace of specular intensity of RHEED during the epitaxial growth of the $[(SZO)_{10}/(STO)_{10}]_4$ superlattice (called as the 10-periodic superlattice hereafter), respectively. The difference in the RHEED intensities of SZO and STO is due to the difference of their reflection intensity of the electron beam. Clear oscillations of the intensity were observed during the growth and these intensity oscillations indicate that the two-dimensional layer-by-layer growth was

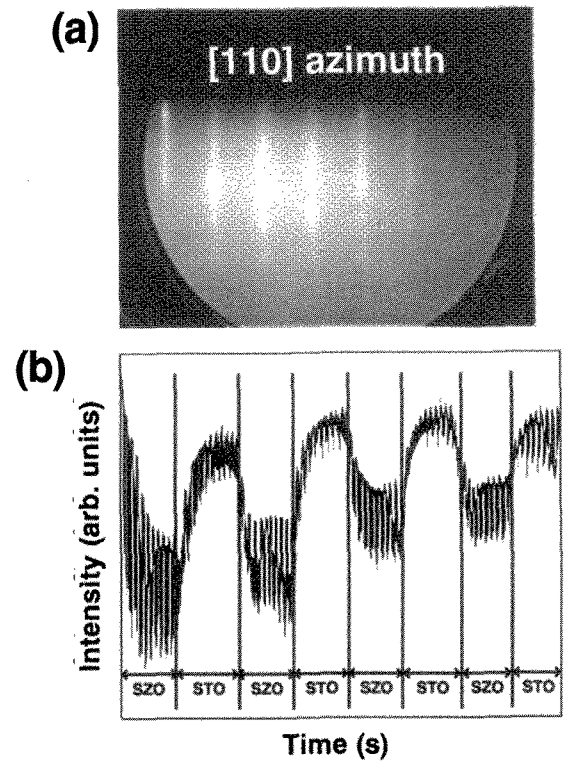

Fig. 1. (a)Profile of RHEED from the [110] azimuth, (b)Trace of specular intensity of RHEED during epitaxial growth of the $[(SZO)_{10}/(STO)_{10}]_4$ superlattice

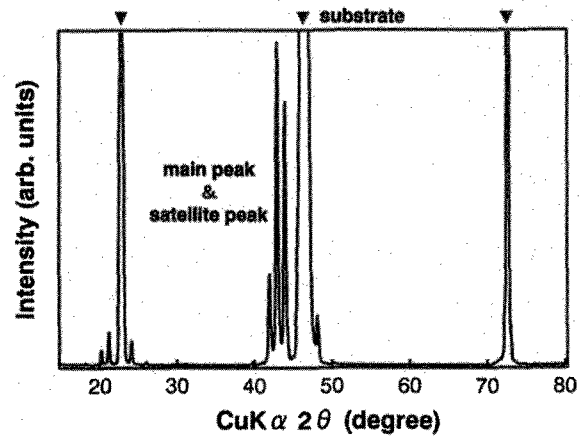

Fig. 2. XRD profile of the $[(SZO)_{10}/(STO)_{10}]_4$ superlattice

achieved in the depositions of the each molecular layer. The XRD profile of the 10-periodic superlattice is shown in Fig. 2. The XRD patterns with several clear satellite peaks are observed at the low angle side of the main peak, and it showed that the SZO/STO superlattices with *(00l)* orientation indicated were successfully prepared. These indicate that almost perfect control was achieved in the atomic-layer epitaxy by the MBE system used in the present study.

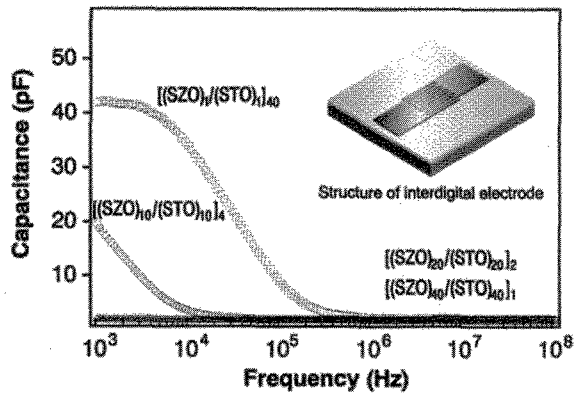

Fig. 3. Capacitance of SZO/STO superlattices with interdigital electrode

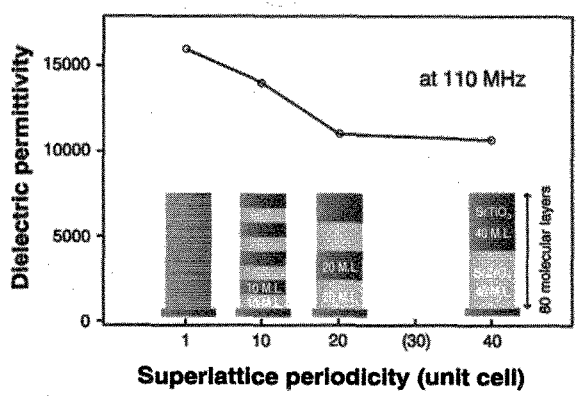

Fig. 4. Dielectric permittivity of SZO/STO superlattices as a function of the periodicity

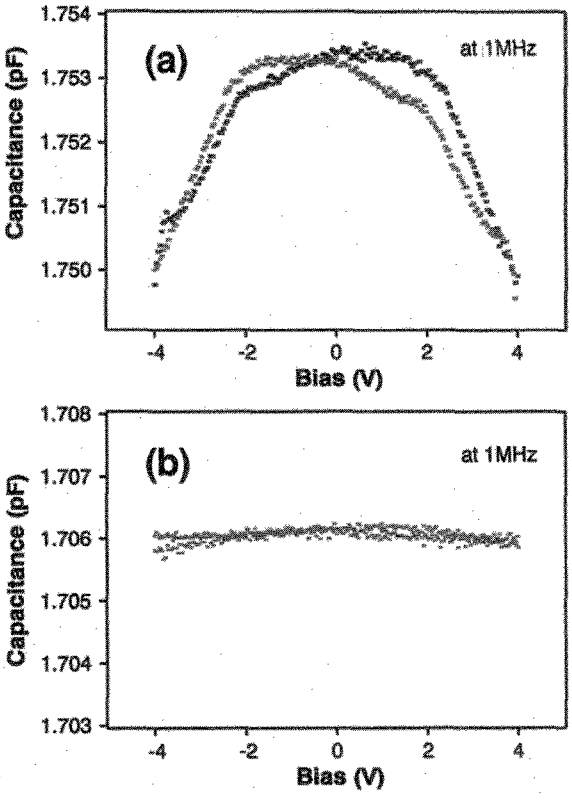

Fig. 5. Capacitance as a function of DC bias voltage for (a) $[(SZO)_{10}/(STO)_{10}]_4$ superlattice and (b) STO.

3.2. Dielectric properties of superlattices

Figure 3 shows capacitances of SZO/STO superlattices as a function of frequency measured with interdigital electrodes. It was found that the capacitances were slightly dependent on the stacking periodicity of superlattices. Moreover, dielectric relaxation was observed with the sample of 1- and 10 -periodic structures in the low frequency domain of 1 MHz or less. In the 1-periodic superlattice, a dielectric loss peak was observed at 250 kHz and the loss increased at frequencies lower than 10 kHz. The increase in the loss at low frequencies was due to the electric conduction. The peak frequency of the dielectric loss of the 10-periodic superlattice was even lower than that of the 1-periodic superlattice. This kind of dielectric relaxation was not observed in the case of BTO/STO superlattices[6].

The dielectric permittivity of the superlattices determined from the complex admittance using the electromagnetic field analysis is shown in Fig. 4. The permittivity of the superlattices at 110 MHz was changed as a function of the period of layers. The minimum permittivity was 10,500 when the superlattice consists of the 40-periodic structures, and the permittivity of the 1-periodic superlattice could not be determined because of its high leakage current. It was found that the permittivity decreased with increasing periodicity over the 10-periodic structure. In the our previous researches[5,6], BTO/STO system showed the giant dielectric permittivity which notably changed with the lamination cycle. However, in the case of SZO/STO system, although its dielectric permittivity was large, the change with the lamination cycle was not so dramatic as that of BTO/STO system. Figure 5 shows capacitance of STO and the 10-periodic superlattice as a function of DC bias voltage at 1 MHz. Although voltage tuning was hardly observed in STO sample, the voltage tunability of the superlattice was significantly increased when a bias of 4 V is applied.

Figure 6 shows Q-V hysteresis of SZO/STO superlattices measured at 132.5 Hz using interdigital electrodes. The 1-periodic superlattice exhibited a round shape, indicating that the films were very leaky. As for the other periodic superlattices, the smaller the period of layers became, the better ferroelectricity with a slim hysteresis loop was observed. Although both of SZO and STO are paraelectricity, the ferroelectricity was discovered in the superlattice which made them to be laminated, and furthermore, the ferroelectricity changed by the lamination cycle.

The origin of the high dielectric permittivity and ferroelectricity with the superlattice structure has not been clearly understood at present, but the authors are considering that the strain induced in the films may play important role to determine the properties. A large distortion was introduced into a hetero interface when the artificial superlattice which laminated the

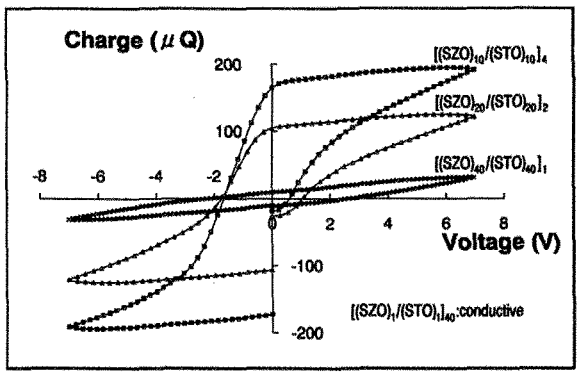

Fig. 6. Q-V hysteresis of SZO/STO superlattices measured using interdigital electrode

substance with which lattice constants differ was produced. In the case of the SZO/STO system, the lattice constant of the bulk of SZO (orthorhombic SZO; a=0.57862, b=0.58151 and c=0.81960 nm[8]) was larger than that of STO (cubic STO; a=0.3905 nm[9]), so that the SZO layer was compressed in the in-plane direction and extended perpendicular to the film plane. As for BTO/STO superlattices, Tabata *et al.*[4] has reported that the pressure induced by the STO layers is estimated to be approximately 400–500 MPa. Abe *et al.*[10-12] was considering how the lattice distortion affects the ferroelectricity of (Ba,Sr)TiO3 epitaxial films using the Devonshire thermodynamic theory[13] and reported that a Curie temperature shifts to the high temperature side rather than original, with the increase in the two-dimensional stress induced in epitaxial films due to the lattice mismatching to the substrate, which was in agreement with their experimental result. Considering the lattice constant of the bulk specimen, the lattice mismatch at the interface between the SZO and STO layers should be larger than the case of the BTO/STO superlattices (tetragonal BTO; a=0.39945, and c=0.40335 nm[14]). The ferroelectricity found in the SZO/STO system was unique in the other sense because it was observed only in the low frequency region accompanied with the dielectric relaxation. In normal ferroelectrics, dielectric relaxation is not observed up to GHz region and ferroelectricity maintains at much higher frequencies. With regard to this discrepancy, we think that the 90-degrees switching of spontaneous polarization restricting the switching speed was involved in the measurement of Q-V characteristics with interdigital electrodes because the applied electric field was perpendicular to the direction of its spontaneous polarization.

The similar ferroelectricity was not observed in the BTO/STO superlattices even though they had ferroelectric BTO as a component. This indicates that the anisotropic lattice distortion, which is lager in the SZO/STO than in the BTO/STO superlattices, is more effective to induce the ferroelectricity than the ferroelectric nature of BTO. The BTO/STO superlattices had less lattice distortion but showed a larger dielectric permittivity in comparison with the SZO/STO superlattices. In the perovskite-type superlattices, a large lattice distortion enhanced the ferroelectricity but reduces the dielectric permittivity, which is analogous in the behaviors of normal ferroelectrics and relaxors.

4. CONCLUSION

In this study, we fabricated the SZO/STO artificial superlattices on STO substrates by the MBE process. Their dielectric properties were measured using interdigital electrodes frequencies up to 110 MHz. Dielectric relaxation was observed in the 1- and 10-periodic superlattices in the low frequency domain of 1 MHz or less. The calculated dielectric permittivity was changed as a function of the stacking periodicity and was over 10,000 with all superlattices at 110 MHz. The 10-periodic superlattice showed a clear hysteresis curve, suggesting that the ferroelectricity was induced into the SZO/STO superlattices although both of SZO and STO showed paraelectricity in nature. It seemed that the anisotropic lattice distortion induced by the lattice mismatch between SZO and STO was the origin of the ferroelectricity.

References

[1] K. Iijima, T. Terashima, Y. Bando, K. Kamigai, and H. Terauchi, J. Appl. Phys. **72**, 2840 (1992).
[2] T. Tsurumi, T. Suzuki, M. Yamane, and M. Daimon, Jpn. J. Appl. Phys., Part 1 **33**, 5192 (1994).
[3] T. Tsurumi, T. Miyasou, Y. Ishibashi, and N. Ohashi, Jpn. J. Appl. Phys.,Part 1 **37**, 5104 (1998).
[4] H. Tabata, H. Tanaka, and T. Kawai, Appl. Phys. Lett. **65**, 1970 (1994).
[5] T. Tsurumi, T. Ichikawa, T. Harigai, H. Kakemoto, and S. Wada, J. Appl. Phys. **91**, 2284 (2002).
[6] T. Harigai, D. Tanaka, H. Kakemoto, S. Wada, and T. Tsurumi , J. Appl. Phys. **94**, 7923 (2003)
[7] G. Farnell, I. Cermak, P. Silver, and S. Wong, IEEE Trans. on Sonics and Ultrasonics, **SU-17**, 188-95(1970).
[8] Ahtee, A. Ahtee, M. Glazer, A.M. Hewat, Phase Transition **38**, 127-220 (1992).
[9] Meyer, G.M.Nelmes, R.J. Hutton, Phase Transition **38**, 127-220 (1992).
[10] K. Abe, S. Komatsu, N. Yanase, K. Sano and T. Kawakubo, Jpn. J. Appl. Phys. **36**, 5575 (1997).
[11] K. Abe, N. Yanase, S. Komatsu, K. Sano and T. Kawakubo, Oyo Buturi **67**, 1286 (1998) [in Japanese].
[12] T. Kawakubo, S. Komatsu, K. Abe, K. Sano, N. Yanase and N. Fukushima, Jpn. J. Appl. Phys. **37**, 5108 (1998).
[13] A. F. Devonshire, Philos. Mag. **40**, 1040 (1949).
[14] Evans, H.T.jr, Phase Transition **38**, 127-220 (1992).

(Received October 11, 2003; Accepted March 10, 2004)